



***In silico* Analysis of the Structural Properties of PSMA and its Energetic Relationship with Zn as Cofactor**

M.A. Fuentes¹, L. A. Mandujano², R. López³, L.R. Guarneros⁴, E. Azorín⁵, D. Osorio-González^{1*}¹*Molecular Biophysics Laboratory of the Faculty of Sciences, Autonomous University of Mexico State, Mexico*²*Molecular Biophysical Modeling and Design Laboratory, Mexiquense University, S. C.*³*Multiscale Molecular Bioengineering Laboratory of the Faculty of Sciences, Autonomous University of Mexico State, Mexico**Email: dog@uaemex.mx

ARTICLE INFORMATION

Received: June 16, 2018

Revised: July 05, 2018

Accepted: July 20, 2018

Published online: August 6, 2018

Keywords:

PSMA structural analysis, PSMA with and without Zn as cofactor.

DOI: [10.15415/jnp.2018.61020](https://doi.org/10.15415/jnp.2018.61020)

ABSTRACT

The prostate-specific membrane antigen (PSMA) is a 100 kDa type II transmembrane glycoprotein with enzymatic activity similar to the family of zinc-dependent exopeptidases. This protein is of great medical and pharmacological interest as overexpression in prostate cells is related to the progression of prostate cancer; therefore, it represents an important target for the design of radiopharmaceuticals. The presence of two Zn²⁺ ions in the active site is crucial to the enzymatic activity and the design of high-affinity inhibitors. The amino acid residues coordinating these ions are highly conserved in PSMA orthologs from plants to mammals, and site-mutagenesis assays of these residues show a loss of enzymatic function or reduction of the kinetic parameters. In the present work, we performed molecular dynamics simulation of PSMA with the purpose of characterizing it energetically and structurally. We elucidated the differences of PSMA with its two Zn²⁺ ions as cofactors and without them in the free energy profile, and in four structural parameters: root mean square deviations and root mean square fluctuations by atom and amino acid residue, radius of gyration, and solvent accessible surface area.

1. Introduction

Prostate cancer is a global problem since it is the second type of cancer with the highest incidence and the fifth with the highest number of deaths among men, while in Mexico it is the cancer type with higher incidence and mortality rate [1]. The Prostate-specific Membrane Antigen (PSMA) is a type II transmembrane glycoprotein of 100 kDa composed of 750 amino acids with at least three functions: hydrolytic NAALADase activity, folate hydrolase and dipeptidyl peptidase IV activity [2-4]. This protein is overexpressed in poorly differentiated and metastatic cells; consequently, it is considered an important indicator of prostate cancer and a target for the development of many inhibitors [5-6]. Recently, small molecule inhibitors (SMI) targeting PSMA have been developed; these are zinc-binding compounds linked to glutamate or a glutamate isomer. Urea-based SMI (Glu-urea-R) have demonstrated to specifically bind to PSMA and inhibit its activity in the LNCaP cell line. In such compounds, Glu-urea is the binding terminal and the R-group is the coupling terminal to other chemical groups such as a linker and a chelator associated with radionuclides [7-10].

The theranostic agents are based on the use of a radionuclide with the same PSMA-targeting ligands for therapy and diagnosis; for this purpose ¹⁷⁷Lu, ²²⁵Ac, and ¹³¹I have been used. Particularly, ¹⁷⁷Lu associated with PSMA-617 has provided a safe and effective therapy in patients with metastatic castration-resistant prostate cancer [11-14]. PSMA-617 is a ligand conformed by a DOTA chelator (1,4,7,10-Tetraazacyclododecane-1,4,7,10-tetraacetic acid) conjugated with Glu-urea-Lys pharmacophore by a linker composed of two aromatic rings; it was designed for labeling with ¹⁷⁷Lu and ⁶⁸Ga to achieve high-quality image and efficient endotherapy [15-16].

Crystallographic structural studies of PSMA made possible to elucidate the interaction of the protein with the inhibitors. Structural information of PSMA is available only for the extracellular part of the protein (residues 44-750). It reveals that the protein exists as a symmetrical homodimer *in vivo*, each polypeptide monomer having three structural domains: a protease-like domain (residues 56-116 and 352-591), an apical domain –also called the protease-associated domain- (residues 117-351), and the helical domain – also called the C-terminal domain- (residues 592-750). [Figure. 1]. The active site of the protein contains a binuclear

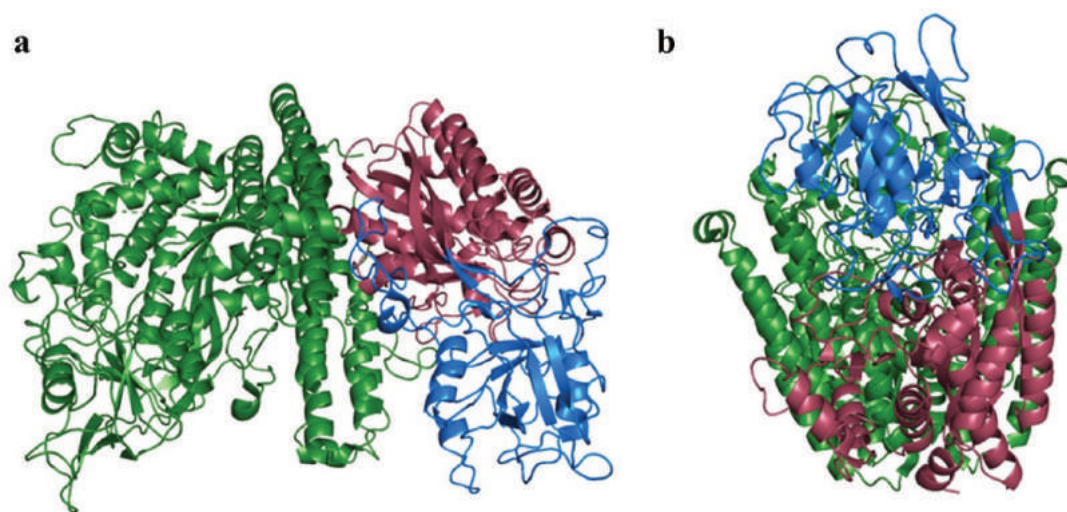


Figure 1. PSMA structural domains. a) lateral view and b) superior view. The protease domain (56-116 and 352-591) is colored in red, the apical domain (117-351) in blue, and the helical domain in green (592-750).

Zn active site, catalytic residues, and a substrate-binding arginine-rich patch. A water ligand bridges the two zinc atoms, each coordinated by endogenous ligands: Zn(1) by His553 and Glu425, Zn(2) by His377 and Asp453, both atoms bounded by Asp387. Glu424 and Tyr552 have the catalytic function. A substrate/inhibitor-binding cavity with an area of about 1100 Å², and a diameter and deep of about 20 Å, is formed in the interface between the three domains; this interface is considered large as it buries around 4600 Å². It is localized in the helical domain and is formed by two pockets, S1' (pharmacophore) and S1 (non-pharmacophore). The cavity has an arginine patch (Arg463, Arg534, and Arg536) involved in the right orientation of the substrate for catalysis; it is aligned with the S1 which has a chlorine ion that keeps Arg534 in a conformation that allows the interaction with the substrate, while Arg536 and Arg463 are flexible conferring tolerance to different chemical groups [Figure 2]. The "glutamate sensor" is responsible of detecting the absence or presence of glutamate in S1' pocket and is formed by residues 692-704 together with Lys699 and Tyr700, which are also important for the specific binding of glutamate along with Arg210 in the apical domain [17-19].

The pharmacophore Glu-urea-Lys (iPSMA) [Figure 3] is capable of binding with PSMA because it has three carboxylic acid groups. The glutamate-urea fraction of the inhibitor has a predisposition to be oriented towards S1', and lysine is used for conjugation or derivatization, through the free amine, with a linker region or a chelating agent residing in S1. When both pockets are occupied, the hydrophobic contact (due to an aromatic agent) increases resulting in higher affinity [20,21]. The affinity to PSMA is due to the binding of glutamate by its α -carboxylate, which

forms a bridge with the guanidinium group of Arg210, and hydrogen bonds with the hydroxide groups of Tyr552 and Tyr700, while the γ -carboxylate interacts with Lys699 and Ans257. The catalytic activity is carried out by Glu424, that extracts a proton from the water molecule situated between the zinc atoms and activates it [19,22]. The urea group serves as a zinc-binding group (ZBG) because the oxygen of the molecule interacts with Tyr552, His553, the active water molecule and Zn(1), while N groups form hydrogen bonds: N(1) with the main carbonyl chain of Gly-518 and the carboxylate of Glu-424, and N(2) with γ -carbonyl of Gly-518 [19, 23-24].

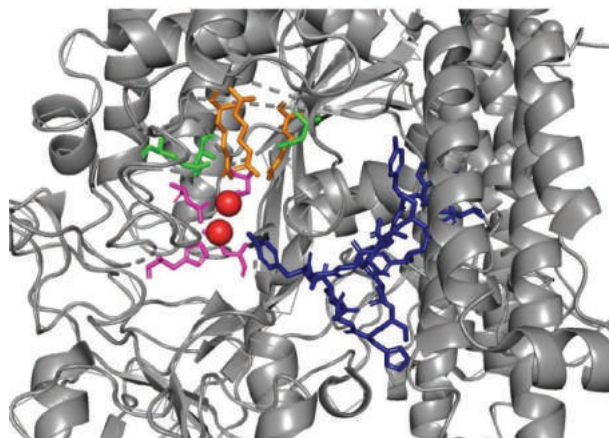


Figure 2. PSMA active site. Zinc ions are observed as red spheres, while the coordinating ligands of these ions are presented as magenta sticks. The substrate binding cavity is colored in blue, the arginine patch in orange and stabilizing ligands in green.

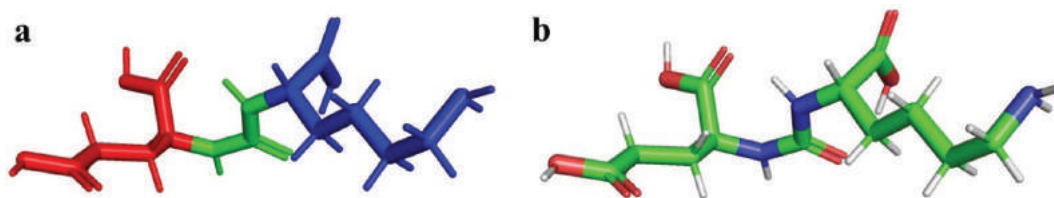


Figure 3. iPSMA structure (Glu-urea-Lys). a) The pharmacophore is composed by a glutamate (red), urea (green) and lysine (blue). b) Oxygen atoms are colored in red sticks, carbon colored in green sticks, hydrogen colored in white sticks and nitrogen colored in blue sticks.

2. Method

2.1 Theoretical model

To evaluate the structure of a biomolecule, we calculate the Root Mean Square Deviation (RMSD) between its atoms or residues, which allows comparing its molecular structure reached at any time t_1 , with respect to another structure that occurred at a reference t_2 , for this purpose we use the expression

$$RMSD(t_1, t_2) = \left[\frac{1}{M} \sum_{i=1}^N m_i \|r_i(t_1) - r_i(t_2)\|^2 \right]^{\frac{1}{2}} \quad (1)$$

Where m_i is the mass of the atom or residue i in the position r_i , and therefore $M = \sum_{i=1}^N m_i$ is the total mass of the system.

It is possible to analyze the flexibility of the protein through the oscillations of its amino acids, this property can be estimated through the Root Mean Square Fluctuation (RMSF) which can be calculated using

$$RMSF(i) = \left[\frac{1}{T} \sum_{t_1=1}^T \|r_i(t_1) - r_i(t_2)\|^2 \right]^{\frac{1}{2}} \quad (2)$$

Where T is the time over which the average is calculated.

To have a rough measure for the compactness of a protein structure, we calculate the radius of gyration with

$$R_g = \left(\frac{\sum_{i=1}^N \|r_i\|^2 m_i}{\sum_{i=1}^N m_i} \right)^{\frac{1}{2}} \quad (3)$$

Where m_i is the mass of atom i and r_i the position of atom i with respect to the center of mass of the molecule.

The Solvent Accessible Surface Area (SASA) of a molecule is the region of its surface that has contact with the solvent and is, therefore, an indicator of the structural changes generated during the folding of the protein because SASA is directly proportional to its free energy.

2.2 Methodology

For *in silico* analysis we used classical Molecular Dynamics (MD), the atomic coordinates for PSMA were extracted from the 1Z8L crystal structure in the Protein Data Bank. The protein was solvated using atomistic TIP3P water in a cubic box with at least 10 Å distance around the complex. We used the CHARMM force field. The two initial stages in the preparation of the systems, the stages of minimization and equilibration, were carried out using the NAMD2.6 program. First, the systems were minimized for 10000 steps, then thermalized for 10 ps at 300 K reinitializing the velocities every 20 ps. The equilibration of the systems was carried out with NAMD2.6 under periodic boundary conditions, time step 2 fs, cutoff 9 Å, Langevin damping 0.1/ps. The long-range electrostatic interactions are accounted for using the particle mesh Ewald method, with a maximum grid spacing of 1.0 Å. Bond lengths are maintained rigid with the SHAKE. A final run of 100 ns was executed to assure that all properties, such as potential energy, van der Waals and electrostatic interactions, are in thermodynamic equilibrium. After 15 ns these quantities remain stable.

After the initial equilibration phase, the production simulation (100 ns) was carried out using platform ACEMD. This simulation was conducted in the NVT ensemble which resulted from the equilibration phase. We use a longer timestep of 4 fs thanks to the use of the hydrogen mass repartition scheme implemented in ACEMD. Coordinate snapshots were generated every 5 ps collecting a total of 5000 conformational states for subsequent post-production analysis. The structural analysis presented in this work was held on 100 ns of simulation time. Molecular images displayed in this work were produced using PyMOL. All simulations referred were performed at our Cluster OLINKA, a platform designed to run molecular simulations to multiscale with GPUs.

3. Results and Discussion

It is noteworthy that the active site is centered around the two zinc ions, and separates the S1' and S1 pockets. One of the Zn^{2+} is considered the catalytic ion, coordinated by His553

and Glu425, and the other is the co-catalytic, coordinated by His377 and Asp453. Asp387 and a water molecule bridge the two zinc atoms thus forming a coordination sphere [19]. These five Zn-coordinating residues were implicated in site-mutagenesis experiments resulting –with exception of the specific Asp387Asn substitution-, in no detectable enzymatic activity or an enzymatic activity too low for determination of kinetic parameters of PSMA mutants. The importance of these amino acids for PSMA activity is further noted in the fact that they are highly conserved in PSMA orthologs from plants to mammals [17,25].

Zn atoms are crucial for the enzymatic function of PSMA and for the design of inhibitors. In fact, the presence of a zinc-binding group is a fundamental feature in the design of high-affinity inhibitors of PSMA; among the substances that exhibit these groups are thiols, phosphonates, hydroxamates, phosphinates, phosphoamidates, ureas, and sulfonamides [19]. Once established the crucial role of Zn atoms, this work elucidates the differences in the free energy profile and four structural parameters of PSMA with the two Zn atoms as cofactors and without them: RMSD and RMSF by atom and amino acid residue, radius of gyration and SASA.

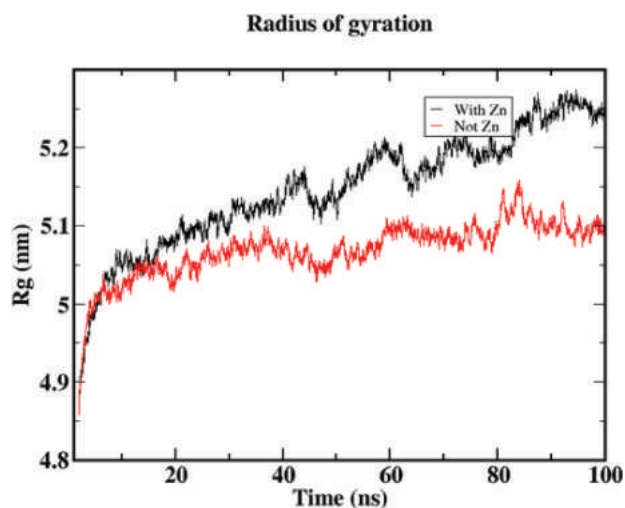


Figure 4. Radii of gyration (Rg) graphic over time showing the results from the simulation of the protein with and without the zinc atoms in the active site.

Radius of gyration gives an idea about the compactability of the molecule during time, since it provides an average of the expansion of its atoms with respect to its center of mass. When comparing the PSMA simulated with and without the zinc ions, it is visible that the PSMA with de zinc ions became more expanded over time than the other [Figure 4], consequently the zinc ions make the structure more receptive to the substrate/inhibitor by adopting an

expanded geometrical conformation that allows its entrance. On the other hand, the RMSF (which is associated with flexibility) shows that the zinc coordinating amino acids of the Zn(1): His-553 and Glu-425, including Asp-387, are more flexible when simulated with the ions, while in the case of Zn(2): His-377 and Asp453 the flexibility is slightly higher [Figure 5]. This information is consistent with the fact that Zn(1) is consider the catalytic ion and as a result the coordinating amino acids need more flexibility for the interaction with the substrate/inhibitor, whilst Zn(2) is considered co-catalytic and the amino acids may not need to be so flexible [19].

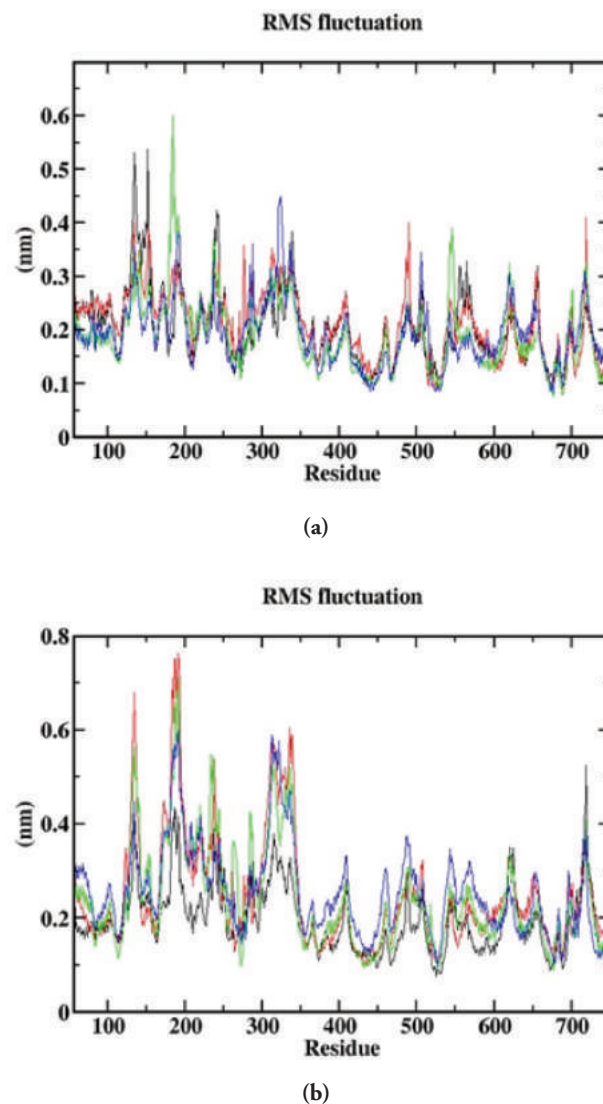


Figure 5. Root Mean Square Fluctuation (RMSF) graphic. The RMSF is related to flexibility and is calculated for each of the amino acids conforming the PSMA, the resulting variations are shown. a) PSMA without zinc and b) PSMA with the zinc ions.

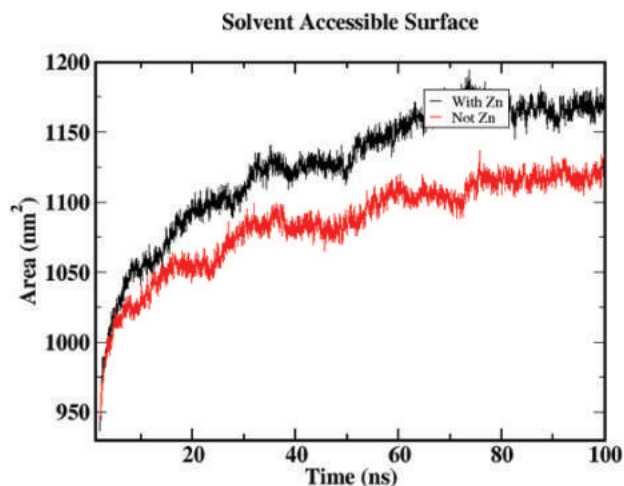


Figure 6. Solvent Accessible Surface Area (SASA) graphic showing the results over time for the PSMA with and without zinc ions.

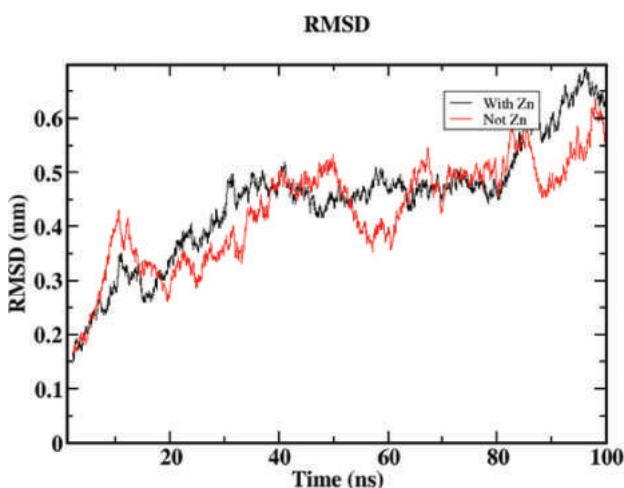


Figure 7. Root Mean Square Deviation (RMSD) graphic. The RMSD is related to structure stability of the atoms or residues over time of PSMA with and without the zinc ions.

In the RSME, significant changes in flexibility between the two conditions are not observed in the substrate binding cavity (residues 687-704) and in the “glutarate sensor” (residues 692-704) indicating that the zinc atoms have no impact in these regions. The same situation was observed in the arginine patch (Arg-534, Arg-536 and Arg-463) meaning that the zinc ions do not play an important role in the right orientation of the substrate/inhibitor since the arginines are responsible of that task [17]. However, in Tyr-552 and Glu-424, to which catalytic activity and substrate recognition have been attributed respectively, more flexibility was observed in PSMA with the zinc ions confirming the significance of the interactions between the zinc ions and these amino acids in the active site [18]. The

results from SASA are consistent with R_g , accordingly with the fact that the PSMA with the zinc ions is more expanded, it also has more solvent accessible surface area conferring it more free energy [Figure 6]. The RMSD shows that the PSMA with the zinc ions has more structural stability as it has less variations during time compared with the simulation without them. Therefore, the zinc ions are important for the structural stability of the protein [Figure 7].

4. Conclusions

In silico analysis of the PSMA showed that its structural stability has a direct and intrinsic dependence of its active center, in fact, the tests performed on the protein excluding the Zn atoms are conclusive to affirm that PSMA not only loses affinity to bind with molecules like inhibitors, also their energy capacity is diminished; however, there are regions between residues 100-122 and 640-730 that exhibit structural stability regardless of the absence of the Zn atoms. The tests carried out on PSMA with and without the heart of its active center, the Zn atoms, allowed us to conceive the protein as a closed system, with less energy and flexibility (in the absence of atoms). This situation is completely opposite when they are incorporated, which can be interpreted that PSMA behaves like a biological trap dependent on Zn. The CHARMM force field used was appropriate for modeling the PSMA interactions and can be adapted to study the processes involved in the active center in the presence of a urea-based inhibitor and, of course, a therapeutic radiopharmaceutical.

Acknowledgments

The authors wish to thank, COPARMEX ESTADO DE MÉXICO and UNIVERSIDAD MEXIQUENSE for scholarship support and Dra. Lorena Romero Salazar from Nanothermodynamics and Complex Systems Laboratory by granting facilities for the timely development of the project.

References

- [1] M. Ervik, F. Lam, J. Ferlay, L. Mery, I. Soerjomataram, F. Bray, *Lyon, France: International Agency for Research on Cancer. Cancer Today*(2016). <http://gco.iarc.fr/today>. Accessed 10 April 2018.
- [2] R. Carter, A. Feldman, J. Coyle, *Proceedings of The National Academy of Sciences*, **93**(2), 749–753 (1996). <https://doi.org/10.1073/pnas.93.2.749>
- [3] M. N. Pangalos J. M. Neefs, M. Somers, P. Verhasselt, M. Bekkers, L. van der Helm *et al.*, *Journal of Biological Chemistry*, **274**(13), 8470–8483 (1999). <https://doi.org/10.1074/jbc.274.13.8470>

- [4] J. T. Pinto, B. P. Suffoletto, T. M. Berzin, C. H. Qiao, S. Lin, W. P. Tong *et al.*, *Clinical Cancer Research*, **2(9)**, 1445–1451 (1996).
- [5] R. Lapidus, C. Tiffany, J. Isaacs, B. Slusher, *The Prostate*, **45(4)**, 350–354 (2000).
[https://doi.org/10.1002/1097-0045\(20001201\)45:4<350::AID-PROS10>3.0.CO;2-U](https://doi.org/10.1002/1097-0045(20001201)45:4<350::AID-PROS10>3.0.CO;2-U)
- [6] J. Troyer, M. Beckett, G. Wright, *International Journal of Cancer*, **62(5)**, 552–558 (1995).
<https://doi.org/10.1002/ijc.2910620511>
- [7] A. P. Kiess, S. R. Banerjee, R. C. Mease, S. P. Rowe, A. Rao, C. A. Foss *et al.*, *European Journal of Nuclear Medicine and Molecular Imaging*, **59(3)**, 241 (2015).
- [8] S. Lütje, S. Heskamp, A. S. Cornelissen, T. D. Poeppel, S. A. van den Broek, S. Rosenbaum-Krumme *et al.*, *Theranostics*, **5(12)**, 1388 (2015).
<https://doi.org/10.7150/thno.13348>
- [9] K. P. Maresca, S. M. Hillier, F. J. Femia, D. Keith, C. Barone, J. L. Joyal *et al.*, *Journal of Medicinal Chemistry*, **52(2)**, 347–357 (2008).
<https://doi.org/10.1021/jm800994j>
- [10] Z. Zhang, Z. Zhu, D. Yang, W. Fan, J. Wang, X. Li *et al.*, *Oncology letters*, **12(2)**, 1001–1006 (2016).
<https://doi.org/10.3892/ol.2016.4699>
- [11] A. Escudero-Castellanos, B. E. Ocampo-García, G. Ferro-Flores, K. Isaac-Olivé, C. L. Santos-Cuevas, A. Olmos-Ortiz *et al.*, *Journal of Radioanalytical and Nuclear Chemistry*, **314(3)**, 2201–2207 (2017).
<https://doi.org/10.1007/s10967-017-5555-9>
- [12] W. P. Fendler, K. Rahbar, K. Herrmann, C. Kratochwil and M. Eiber, *Journal of Nuclear Medicine*, **58(8)**, 1196–1200 (2017).
<https://doi.org/10.2967/jnumed.117.191023>
- [13] C. Kratochwil, F. Bruchertseifer, F. L. Giesel, M. Weis, F. A. Verburg, F. Mottaghy *et al.*, *Journal of Nuclear Medicine*, **57(12)**, 1941–1944 (2016).
<https://doi.org/10.2967/jnumed.116.178673>
- [14] C. M. Zechmann, A. Afshar-Oromieh, T. Armor, J. B. Stubbs, W. Mier, B. Hadaschik *et al.*, *European Journal of Nuclear Medicine and Molecular Imaging*, **41(7)**, 1280–1292 (2014).
<https://doi.org/10.1007/s00259-014-2713-y>
- [15] M. Benešová, M. Schäfer, U. Bauder-Wüst, A. Afshar-Oromieh, C. Kratochwil, W. Mier *et al.*, *Journal of Nuclear Medicine*, **56(6)**, 914–920 (2015).
<https://doi.org/10.2967/jnumed.114.147413>
- [16] C. Kratochwil, F. L. Giesel, M. Eder, A. Afshar-Oromieh, M. Benesová, W. Mier *et al.*, *European Journal of Nuclear Medicine and Molecular Imaging*, **42(6)**, 987 (2015).
<https://doi.org/10.1007/s00259-014-2978-1>
- [17] M. I. Davis, M. J. Bennett, L. M. Thomas, P. J. Bjorkman, *Proceedings of the National Academy of Sciences*, **102(17)**, 5981–5986 (2005).
<https://doi.org/10.1073/pnas.0502101102>
- [18] J. R. Mesters, C. Barinka, W. Li, T. Tsukamoto, P. Majer, B. S. Slusher *et al.*, *The EMBO journal*, **25(6)**, 1375–1384 (2006).
<https://doi.org/10.1038/sj.emboj.7600969>
- [19] J. Pavlicek, J. Ptacek, C. Barinka, *Current Medicinal Chemistry*, **19(9)**, 1300–1309 (2012).
<https://doi.org/10.2174/092986712799462667>
- [20] S. R. Banerjee, C. A. Foss, M. Castanares, R. C. Mease, Y. Byun, J. J. Fox *et al.*, *Journal of Medicinal Chemistry*, **51(15)**, 4504–4517 (2008).
<https://doi.org/10.1021/jm800111u>
- [21] S. M. Hillier, K. P. Maresca, F. J. Femia, J. C. Marquis, C. A. Foss, N. Nguyen *et al.* *Cancer Research*, **69(17)**, 6932–6940 (2009).
<https://doi.org/10.1158/0008-5472.CAN-09-1682>
- [22] P. Mlčochová, A. Plechanovova, C. Bařinka, D. Mahadevan, J. W. Saldanha, L. Rulíšek, J. Konvalinka, *The FEBS Journal*, **274(18)**, 4731–4741 (2007).
<https://doi.org/10.1111/j.1742-4658.2007.06021.x>
- [23] C. Barinka, Y. Byun, C. L. Dusich, S. R. Banerjee, Y. Chen, M. Castanares *et al.*, *Journal of Medicinal Chemistry*, **51(24)**, 7737–7743 (2008).
<https://doi.org/10.1021/jm800765e>
- [24] D. Ferraris, K. Shukla, T. Tsukamoto, *Current Medicinal Chemistry*, **19(9)**, 1282–1294 (2012).
<https://doi.org/10.2174/092986712799462658>
- [25] H. S. Speno, R. Luthi-Carter, W. L. Macias, S. L. Valentine, A. R. Joshi, J. T. Coyle, *Molecular Pharmacology*, **55(1)**, 179–185 (1999).